Preprint
UCRL-JC-143745

Position Resolution Studies with MSU 32-fold Segmented HPGe Detector

C. E. Lehner, K. Vetter, A. Kuhn, G. J. Schmid, D. A. Beckedahl, J. J. Blair, J. E. Kammeraad, T. Glasmacher

U.S. Department of Energy

Lawrence
Livermore
National
Laboratory

This article was submitted to
Institute of Electrical and Electronics Engineers Nuclear Science Symposium, San Diego, CA, November 5-10, 2001

October 25, 2001

This work was performed under the auspices of the United States Department of Energy by the University of California, Lawrence Livermore National Laboratory under contract No. W-7405-Eng-48.

Position resolution studies with MSU 32−fold segmented HPGe detector

C.E. Lehner, K. Vetter, A. Kuhn, G.J. Schmid, D.A. Beckedahl, J.J. Blair, J.E. Kammeraad, T. Glasmacher

***Abstract*−−We present position sensitivity measurements obtained with one of the 32−fold segmented HPGe detectors from Michigan State University. These measurements were performed with a collimated beam of ^{137}Cs gamma rays scattered by 90 degrees. This deposits 374 keV at a given location inside the crystal. A position resulution can be determined over many events by examining the digitally recorded pulse shapes on the 32 electrical contacts. If position resolution is adequate, gamma ray Compton camera imaging may be possible.**

I. Introduction

For the last several years, we have been studying position resolution in commercial segmented high−purity germanium (HPGe) gamma ray detector systems [1],[2]. Segmented detectors have applications in both nuclear physics experiments and in gamma ray imaging using Compton methods. We discuss here the program to measure position resolution in one of the 32−fold segmented HPGe detectors from MSU, shown in Fig. 1 with the preamplifier covers removed. This detector, manufactured by Eurysis in Cedex, France, was designed for in−beam gamma ray spectroscopy at the National Superconducting Cyclotron Laboratory at MSU. The segmentation scheme allows for a position−dependent Doppler correction to be applied, yielding better energy resolution and cleaner gamma ray spectra.

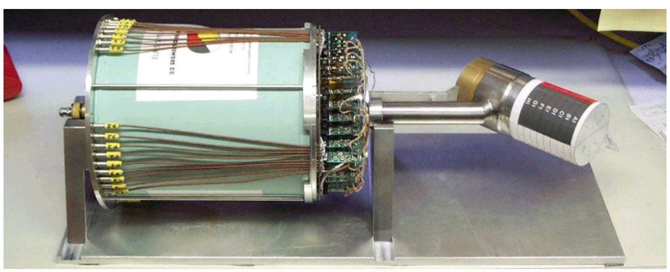

Fig. 1. The MSU detector. The preamplifier covers have been removed. The canister is set at a 45 degree angle to the dewar to allow close packing of several detectors without dewar interference.

As we have shown in our previous work, position resolution can be much smaller than segment size if digital pulse shape analysis is used. We discuss here the best 3−D position resolution achievable in the MSU detector and how that resolution varies with location in the crystal. With good position resolution, it may be possible to determine the location of the first gamma ray interaction in the detector, further improving the Doppler correction for in−beam experiments. Additionally, Compton imaging could be performed if position resolution is sufficiently small.

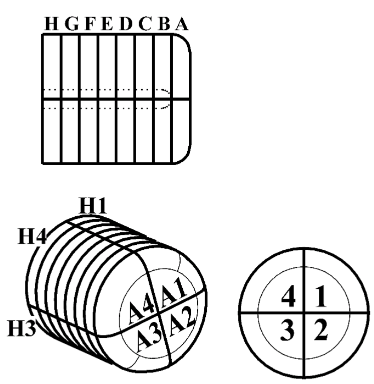

Fig. 2. Segmentation scheme of the MSU detector. There are eight longitudinal and four angular sections for a total of 32 segments.

This research was performed at the UC LLNL and LBNL under the auspices of the US DOE under contract W−7405−Eng−48, and under appointment to the US DOE Nuclear Engineering and Health Physics Fellowship Program sponsored by the DOE Office of Nuclear Energy, Science, and Technology.

II. MSU Segmented Detector

The MSU detector is a closed−ended coaxial n−type HPGe detector. It is 80 mm in length, 70 mm in diameter, and has a bevelled front edge. The segmentation scheme is shown in Fig. 2. The outer contact is segmented into 8 longitudinal and 4 angular sections for a total of 32 segments.

The FETs are warm during operation. The can is angled 45 degrees from the dewar, so that several of these detectors can be placed in close proximity without interference from the dewars. In beam experiments, the side of the detector, not the closed ended front, face the incident radiation.

III. Calculated Signals

Using digital techniques, position resolution can be calculated from knowledge of pulse shapes from each segment. We present first the calculations, and in the next section the measured signals.

To calculate the expected pulse shapes from the collecting and noncollecting electrodes we apply Ramo's theorem [3] for weighting potentials. It is necessary to determine the electric field throughout the detector under operating conditions, as well as the weighted potentials for each segment. Maxwell 3D was used to simulate the electric field in the detector, assuming a nominal space charge of 0.002 C/m^3, corresponding to an impurity density of about 10^{10} cm^{-3}. The exact distribution of space charge in the crystal is not known, and the value above is assumed to be constant throughout. The electric field through the center slice of the C segments is plotted in Fig. 3.

The weighting potentials were then calculated by setting the potential of one segment to 1 V and all other contacts to 0 V. The space charge was excluded in the calculations. The weighting potential through the center slice of the C segments is shown in Fig. 4.

We calculated expected signals from the electric field and weighting potentials as in [1]. Further, these signals were convolved with the measured preamplifier responses. A square wave with 5 ns rise time and 4 ?s period was sent into the test input of the detector, and the corresponding output signals were read from the segments. The preamplifier repsonses were determined by deconvolving the input and output signals without filtering.

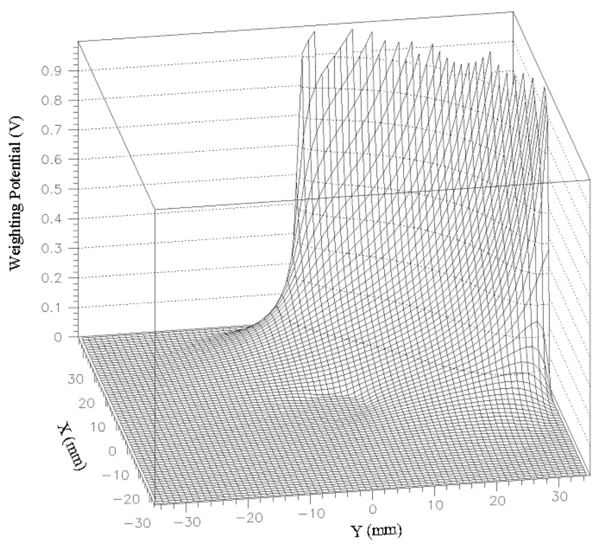

Fig. 4. Simulated weighting potential in the center slice (z=25) of segment C2., calculated by setting C2 to 1 V and all other contacts to 0 V. Granularity is due to the finite grid size on which the potential is calculated.

IV. Measured Signals

To benchmark these calculations it is necessary to measure the signals corresponding to interactions at particular sites and compare the results with calculations. A collimated ^{137}Cs source was placed in front of the detector, determining interaction position in two dimensions. The gamma rays which scattered at approximately 90 degrees were collimated in the third dimension before being absorbed in a NaI detector. The NaI detector was 12.7 cm (5 in) in diameter and 15.2 cm (6 in) in length. Coincident events between the HPGe and NaI detectors triggered the digitization of signals. To reduce background coincidences, an energy gate around 374 keV was used on the HPGe signals, implying a 90 degree scatter event. Using the 1 mm collimators and a source activity of 1 mCi, we obtain a count rate of about 1 event every 10 minutes if the interaction is near the edge of the crystal, or every 30−60 minutes if the interaction is deeper inside the crystal.

The signals were fed into a fast amplifier and then a waveform digitizer with a sampling rate of 500 MHz. The central contact (full energy), NaI coincidence, and coincidence timing signals were also digitized. Data was acquired for segment

C2 in 24−hour intervals at 16 (x,y) locations for 2 (z) depths. The first depth is 1mm away from the B−C segment boundary, and the second is halfway through C2. The interaction locations are shown in Fig. 5.

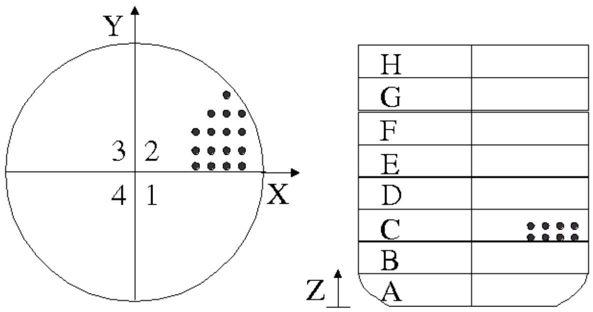

Fig. 5. Locations of interactions for calculated pulse shapes.

Figs. 6 and 7 shows the calculated and measured pulse shapes for two points located 1 mm from the B2 boundary. The signals in Fig. 6 are from a point near the C1 boundary, and those in Fig. 7 correspond to a point in the middle of the C2 segment. Shown in Figs. 8 and 9 are the same points at the second depth.

The calculated signals match fairly well with measured signals, with the exception of B2. The calculated transient signals have a larger amplitude than the measured signals at both points near the B segment boundary. This is not observed consistently for the other spectator signals. It cannot be due to errors in alignment, because the reverse effect is not observed in the D segments.

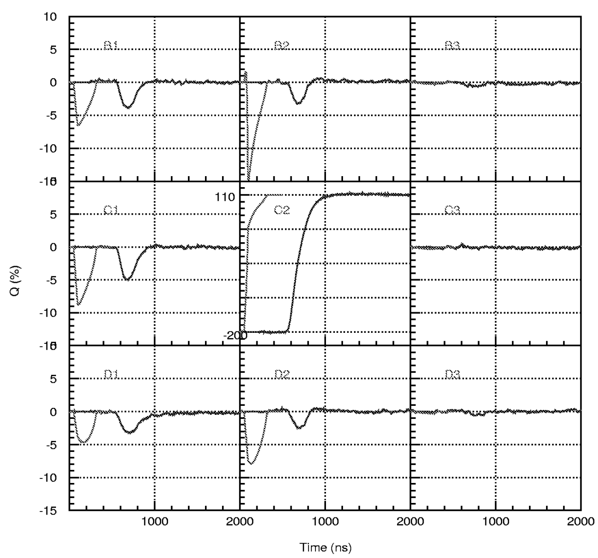

Fig. 6. Measured and calculated pulse shapes in C2 near the C1 boundary at x=30, y=5, z=21.

Fig. 7. Measured and calculated signals in the middle of C2 at x=25, y=20, z=21.

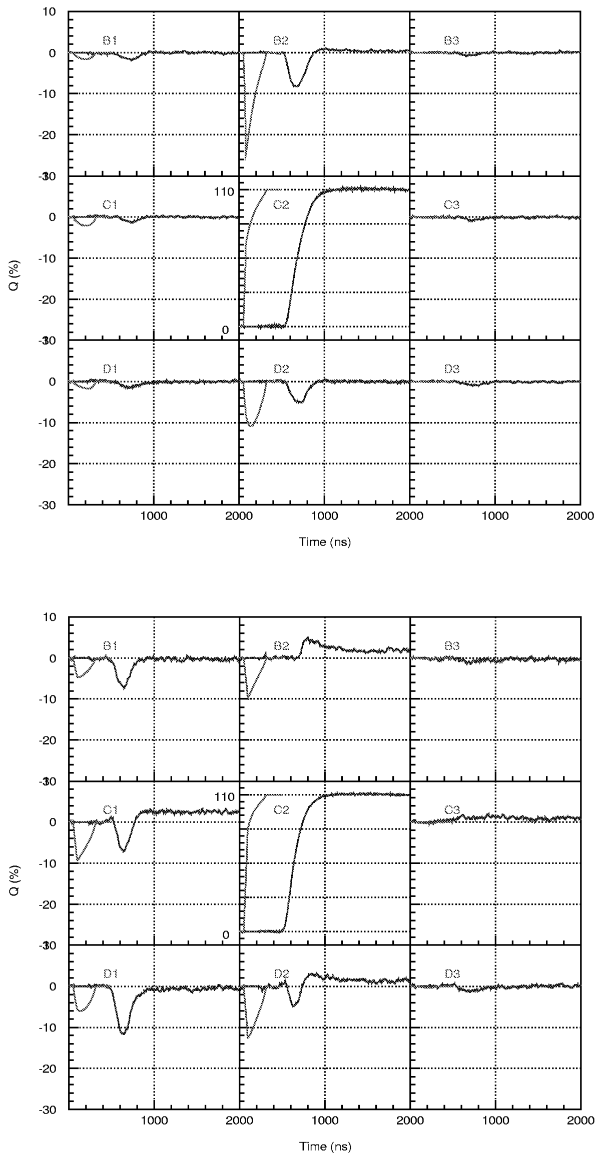

Fig. 8. Same as in Fig. 6 except z=25.

However, the expected trends are observed. There is a larger spectator signal on the nearer angular neighboring segments (e.g. the amplitude of D1 is larger than D3). Additionally, in Figs. 6 and 7 the B segments have larger signals than the D segments, as expected for an interaction near the B−C boundary. The amplitude of the C1 signal does not change with depth of interaction, although the induced signal on D2 is 50% larger at (25,21) than at (31,5) for both depths.

V. Position Resolution

Position sensitivity was calculated as in [1]. The noise level was measured to be about 6 keV for all segments, and this constant value was used in the calculations. The minimum and maximum sensitivities calculated were X and Y.

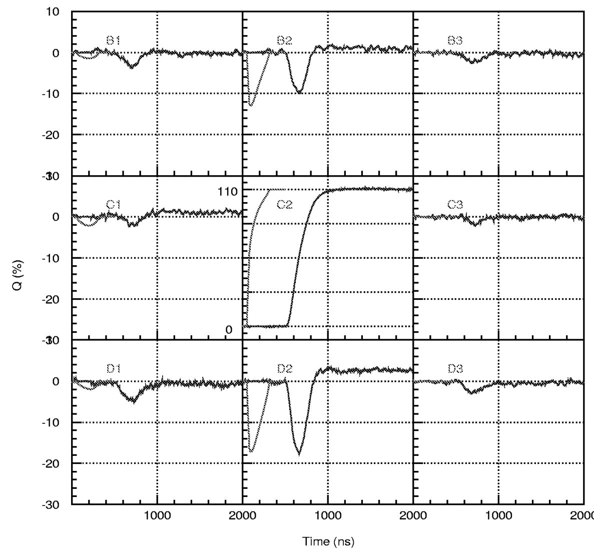

Fig. 9. Same as in Fig. 7 except z=25.

VI. Conclusions

We have performed measurements and calculations to study position resolution in the MSU 32−fold segmented HPGe detector. Calculations reasonably predicted the signals in single−multiplicity events. Position sensitivity was found to be poor, and is not good enough in this detector to perform Compton imaging. To achieve any reasonable image resolution in the reconstruction process, the position resolution in the detector must be much smaller (sub−millimeter if possible).

VII. References

[1] K. Vetter, A. Kuhn, M.A. Deleplanque, I.Y. Lee, F.S. Stephens, G.J. Schmid, et al., "Three−dimensional position sensitivity in two−dimensionally segmented HP−Ge detectors," in Nucl. Instr. Meth. A, vol. 452, pp. 223−238.

[2] G.J. Schmid, D.A. Beckedahl, J.E. Kammeraad, J.J. Blair, K. Vetter, A. Kuhn, "Gamma−ray Compton camera imaging with a segmented HPGe," in Nucl. Instr. Meth. A, vol. 459, pp. 565−576.

[3] S. Ramo, Proc. IRE 27(1939) 584.

[4]